Massive volcanic SO_2 oxidation and sulphate aerosol deposition in Cenozoic North America

Huiming Bao* (bao@lsu.edu)

Department of Geology and Geophysics, Louisiana State University, Baton Rouge, LA 70803-4101, USA

Shaocai Yu* (yu.shaocai@epa.gov)

Atmospheric Modeling and Analysis Division (E243-03), National Exposure Research Laboratory, U.S. Environmental Protection Agency, RTP, NC 27711, USA

Daniel Q. Tong

Air Resources Laboratory, National Oceanic and Atmospheric Administration, Silver Spring, MD 20910, USA

* Corresponding author

Volcanic eruptions release a large amount of sulphur dioxide (SO_2) into the atmosphere[1,2]. SO_2 is oxidized to sulphate and can subsequently form sulphate aerosol or as part of dissolved ions in rain [3], which can affect Earth's radiation balance, biologic productivity and high-altitude ozone concentrations, as evident from recent volcanic eruptions[4]. SO_2 oxidation can occur via several different pathways that depend on its flux and the atmospheric conditions[3]. An investigation into how SO_2 is oxidized to sulphate, the oxidation product preserved in the rock record, can therefore shed light on past volcanic eruptions and atmospheric conditions. Here we use sulphur and triple oxygen isotope measurements of atmospheric sulphate extracted from tuffaceous deposits to investigate the specific oxidation pathways from which the sulphate was formed. We find that seven eruption-related sulphate aerosol deposition events have occurred during the mid-Cenozoic (34 to 7 million years ago) in the northern High Plains, North America. Two extensively sampled ash beds display a similar sulphate mixing pattern that has two distinct atmospheric secondary sulphates. A 3-dimensional atmospheric sulphur chemistry and transport model study reveals that the observed, isotopically discrete sulphates in sediments can be produced only in initially alkaline cloudwater that favours an ozone-dominated SO_2 oxidation pathway in the troposphere. Our finding suggests that, in contrast to the weakly acidic condition today[5], cloudwater in the northern High Plains may have been frequently alkaline during the mid-Cenozoic. We propose that atmospheric secondary sulphate preserved in continental deposits represents an unexploited geological archive for atmospheric SO_2 oxidation chemistry linked to volcanism and atmospheric conditions in the past.

A close temporal correlation between Large Igneous Provinces (LIPs) and major mass extinction events over the last 300 million years implies a potentially causal relationship between the two[6]. Speculation has been on the large amount of gases, including CO_2, SO_2, and halogens that LIPs could have released into the atmosphere and their secondary effects[2]. Despite the immense mass of CO_2 released by LIPs, the added CO_2 is negligible compared to the large atmospheric CO_2 pool[2]. The answer, therefore, might be in the SO_2 flux and its subsequent oxidation, which will affect the thickness and residence time of sulphate aerosol layer and impact the overall oxidizing capacity of the atmosphere [2,7]. While the stratospheric sulphate aerosol might impact more on global climate on a longer time scale, volcanic SO_2 in the troposphere can have much more acute local and regional impacts on environments and society, as recorded by the 1783 Laki basaltic eruption and the subsequent "dry fogs" in continental Europe[8].

Past eruption events offer us a window into exploring the role volcanic SO_2 has played in impacting climate and environment. Most information, such as effects on precipitation and temperature are, unfortunately, not directly recorded for events in the distant past. However, sulphate, the oxidation product, can be preserved in geological records as minerals or in ice cores. Since SO_2 oxidation can take many different pathways that depend on the nature of eruption and initial atmospheric conditions, an investigation into how SO_2 was oxidized to sulphate and subsequently recorded in rock records can shed light on past volcanic eruptions and the atmospheric conditions. Unfortunately, direct observational studies on chemical evolution of SO_2 in volcanic plumes are rare even for modern active eruptions (see ref[9,10]for exception).

Unique insights into current and past atmospheric processes can often be obtained from multiple stable isotope studies of atmospheric species (e.g. NO_3^- in ref[11]). The oxygen in sulphate is derived from water, O_2, and/or O_3 (and its associated compound such as H_2O_2). Triple

66 oxygen isotope and sulphur isotope measurements of atmospheric sulphate can reveal specific
67 oxidation pathways from which the sulphate is formed, in this case, from volcanic SO_2. Bao et
68 al[12,13] first identified highly positive ^{17}O anomalies ($\Delta^{17}O$ value up to +5.84‰) in sulphate
69 extracted from an Oligocene (~28 Myrs ago) ash bed (the mid-Gering ash) near the base of the
70 Arikaree Group, western Nebraska, U. S. A. It was proposed that a massive amount of SO_2 was
71 oxidized to sulphate in the lower troposphere, which was deposited and quickly cemented in ash
72 beds. An extreme sulphate aerosol or "dry-fog" event associated with a volcanic eruption to the
73 west (Colorado), more severe than the 1783 Laki one, was envisaged[13,14]. $\Delta^{17}O$-positive sulphate
74 has also been identified in more recent volcanic ash beds, but with much smaller ^{17}O
75 anomalies[15]. A stratospheric SO_2 + ·OH oxidation may also produce sulphate with highly
76 positive ^{17}O anomalies[16], as observed from volcanic sulphate preserved in recent ice core
77 records[17]. The large quantity of gypsum in the Gering ash bed suggests, however, that the
78 deposited sulphate was mostly formed within the planetary boundary layer (PBL) or lower
79 troposphere, as stratospheric sulphate would be dispersed all over the globe and unlikely to
80 contribute to the concentration level seen in the ash bed. Until this study, the $\Delta^{17}O$-highly-
81 positive mid-Gering sulphate has remained a singular case in geologic records and its origin a
82 mystery.

83 We conducted an extensive survey of the Cenozoic continental deposits in the northern
84 High Plains, including northwestern Nebraska, western South Dakota, and eastern Wyoming
85 (Fig. 1). In addition to the mid-Gering ash, we have found two other ash beds that have sulphate
86 $\Delta^{17}O$ values higher than +5.0‰ in the Arikaree group section exposed in Scotts Bluff National
87 Monument. A total of seven ash-rich, well-cemented tuffaceous beds, five in the Oligocene
88 between 34 and 22 Myrs ago and two in the Miocene Ogallala Group between 7 and 13 Myrs

ago, have been found to have sulphate $\Delta^{17}O$ value higher than +1.4‰ (Fig. 1 & Supplementary Information (SI)). Two distinct ash beds, the "J Ash" (~34 Myrs ago) in the White River Group and the mid-Gering ash (~28.0 Myrs ago) in the Arikaree Group have been extensively sampled from different outcrops in the field and analyzed for $\delta^{34}S$, $\delta^{18}O$, and $\Delta^{17}O$ values in the laboratory.

The $\Delta^{17}O$–$\delta^{18}O$–$\delta^{34}S$ plots for the mid-Gering and the "J ash" beds reveal extremely heterogeneous data for sulphates in a single ash bed; yet all data seem to fall within a triangle defined by three sulphate end-members. We treated the data with a self-consistent Weighted Least Squares method[18] assuming a conservative mixing and a sum of one for all end-members (SI). We obtained for both ash beds a three-end-member mixing scenario as the best fit. Note that there are two atmospheric secondary sulphate end-members in each ash bed (Fig. 2, Table S4).

End-member 1 (E1): a basket for sulphates with no ^{17}O anomaly, including sulphate formed via tropospheric ·OH oxidation or metal-catalyzed O_2 oxidation, and/or from subsequent oxidation of directly deposited SO_2 on surface. Also included is later groundwater sulphate introduced during cementation or calcification. Further apportionment of these sources is difficult within E1, but a dominance by groundwater sulphate is consistent with its higher $\delta^{34}S$ and $\delta^{18}O$ values than those of the two atmospheric secondary sulphate end-members (below).

End-member 2 (E2): atmospheric secondary sulphate from the oxidation of SO_2 via one set of oxidants, less dominated by the O_3 pathway. Only H_2O_2 and O_3 are known oxidants to have positive ^{17}O anomalies in the troposphere[16,19]. The H_2O_2 has $\Delta^{17}O$ values ranging from ~+1 to +2‰[20], while the O_3 from +20 to +35‰[21]. Thus, lower $\Delta^{17}O$ value for sulphate suggests less involvement of O_3 pathway during SO_2 oxidation in the atmosphere. Interestingly, both ash beds share an E2 with almost the same $\Delta^{17}O$–$\delta^{18}O$–$\delta^{34}S$ values (Figure 2, Table S4).

End-member 3 (E3): atmospheric secondary sulphate from the oxidation of SO_2 via another set of oxidants, with higher contribution from the O_3 pathway than in E2. The highly positive $\Delta^{17}O$ value for E3 suggests that O_3 was the dominant oxidant. E3 in the two ash beds is different mainly in the magnitude of the $\Delta^{17}O$. At no other places have we seen the $\Delta^{17}O_{SO4}$ reaches as high as ~ +6‰, neither in any modern atmospheric sulphate[22,23], nor in other ancient volcanic ashes[15,24] or in soils or snow packs of the Antarctica[25,26].

Both E2 and E3 have $\delta^{34}S$ values close to that of magmatic sulphur (~0‰), which is consistent with an origin via direct oxidation of volcanic SO_2. E2 (less O_3-dominated) has a lower $\delta^{18}O$ value (~+2‰) than that of E3 (O_3-dominated) (~+11‰), which is consistent with a high $\delta^{18}O$ value for O_3 (from ~+95 to +125‰) (the $\delta^{18}O$ value for H_2O_2 ranging from +21.9 to +52.5‰)[20,21].

Since late Eocene (~40 Myrs ago), volcaniclastic or tuffaceous deposits have replaced Paleocene-Eocene paleosol-rich deposits and become an important component of the continental deposits in the northern High Plains, North America. This shift in sedimentation coincides with the onset of many silicic volcanic centers developed in the western U. S. during the mid-Tertiary as part of the so-called "ignimbrite flare-ups"[27]. Our data show that late Eocene and early Oligocene had more frequent, $\Delta^{17}O$-highly-positive sulphate-aerosol events than any other time periods of the Cenozoic in the northern High Plains. It is likely that the two Ogallala ash beds have a different volcanic center (Snake River) than that of the White River and the Arikaree ones (Southern Rockies).

In the troposphere, aqueous H_2O_2 and O_3 oxidation of SO_2 can generate sulphate with $\Delta^{17}O$ values as high as +1.2‰ and +8.0‰, respectively[28]. But these two pathways have to compete with other oxidation paths that produce sulphate with $\Delta^{17}O$ ~0. If we were able to sample

atmospheric sulphate in infinitely small space-time windows, we should always be able to pick up the two end members in any SO_2 emission event or even in the background. However, an ash bed is a medium in which atmospheric sulphate was deposited and preserved over a period of time and our sampling and laboratory procedure further mix sulphates of different origins. The fact that our integrated sulphate samples still display two $\Delta^{17}O$-positive sulphate end-members requires that there were time windows in which one O_3-dominated and one less-O_3-dominated pathways produced large fluxes of sulphate, large and temporally separate enough to exert discrete imprints in rock records.

To examine this possibility, especially the existence of a time window in which a large quantity of sulphate can be produced by a O_3-dominated pathway as seen in the mid-Gering case, we ran a 3-dimensional atmospheric sulphur chemical-transport model [U.S. EPA Models-3/Community Multiscale Air Quality (CMAQ)][29] that utilizes existing meteorological fields in western Nebraska and a pre-industrial background sulphur budget for a case of volcanic SO_2 emission from north-central Colorado. The model has the advantage of tracking sulphate chemical productions from the gas-phase ·OH oxidation and five aqueous-phase chemical reactions including aqueous O_3 and H_2O_2 pathways that produce $\Delta^{17}O$-positive sulphate (SI). In this model, we are looking at sulphate deposition during a 13-day period in western Nebraska as the result of a continuous SO_2 emission in the troposphere. We have run model simulations with various combinations of variables, including SO_2 emission rate (5000-ton to 5-million-ton/day), emission type (point source or dispersed over a column), meteorology (summer and winter), dissolved $[Fe^{2+}]$ and $[Mn^{2+}]$ content (e.g. 10^{-10}, 10^{-5}, and 10^{-2} $\mu g/m^3$), initial cloudwater pH (4, 6, 7, 8, and 9 set by background $[Ca^{2+}]$), and stratospheric addition of O_3 via tropopause folding.

157 Total sulphate $\Delta^{17}O$ is calculated assuming sulphate derived from H_2O_2, O_3, and the other
158 pathways contribute +1.2‰, +8.0‰, and 0.0‰, respectively (SI).
159 Model results show that, other variables fixed, higher emission rates usually result in lower
160 bulk sulphate $\Delta^{17}O$ value. Reduced [Fe^{2+}] and [Mn^{2+}] or stratospheric input of O_3 via tropopause
161 folding helps to increase the total sulphate $\Delta^{17}O$ value, but only slightly in an acidic cloudwater
162 condition. Winter, a season with lower overall oxidizing capacity, produces far less sulphate than
163 summer (SI). The model consistently demonstrates that many combinations of variables can
164 convert a large quantity of volcanic SO_2 to sulphate that has a bulk $\Delta^{17}O$ value ranging from +0.5
165 to +2.0‰. Thus, it is not difficult to produce the observed sulphate E2 in the two extensively
166 sampled ash beds (the mid-Gering and the "J") or the $\Delta^{17}O$-positive sulphate observed in 3 of the
167 7 ash beds in Cenozoic North America (Table S1). The problem is for E3 or the $\Delta^{17}O$-highly-
168 positive sulphate in many ash beds. We found that the only scenarios from which the model can
169 produce a large flux of atmospheric secondary sulphate with a highly positive $\Delta^{17}O$ are the ones
170 with alkaline background cloudwater pH (Fig. 3). Note that upon the injection of massive SO_2
171 and its subsequent oxidation to H_2SO_4, the cloudwater pH will inevitably decrease over time. It
172 is the initial background cloudwater pH that exerts a critical role. This is due to the fact that the
173 rate of aqueous O_3 pathway overwhelms those of other competing paths only at higher pH^3. High
174 cloudwater pH in combination with an overall low oxidizing capacity (such as the winter
175 meteorological condition) is shown to be the ideal scenario to produce sulphate that is 1) high in
176 flux, 2) highly positive in the $\Delta^{17}O$, and 3) discrete in time (Fig. 3). These are the three
177 conditions required to explain the observed two atmospheric secondary sulphate end-members in
178 the Wildcat Ridge (~28 Myrs ago) or the Pete Smith Hill (~34 Myrs ago) ash beds.

Alkaline condition is rare in modern atmosphere, except for places of pristine conditions or rich in alkaline dust (e.g. ref.[30]). Modern rainwater pH is mostly below 7 in western Nebraska (SI), which could not produce the observed sulphate deposition pattern as shown by our modeling results. Our finding implies that the cloudwater pH in the northern High Plains of North America was alkaline at the onset of at least two major explosive volcanic eruptions in the mid-Cenozoic (~28Ma and ~34Ma). This further suggests that, differing from its modern weakly acidic condition, this region may have had frequent alkaline couldwater conditions in the mid-Cenozoic. The different $\Delta^{17}O$ values for E3 in the two ash beds (i.e. +2.9 vs. +6.0‰) also suggest that the alkaline condition itself had variable capacities. A frequent alkaline cloudwater condition in the past, therefore, provides a new reference for gauging anthropogenic impact of the atmosphere. An alternative, yet more speculative scenario is that the roof rocks (e.g. carbonates and/or calcareous shales) of the volcanoes may have played a role in increasing cloudwater pH value, through physical dispersion of Ca-rich dust particles, part of which may possibly be CaO formed by thermal decomposition of $CaCO_3$. In recent years, new satellite observational tools have just begun to look into the physical and chemical evolution of volcanic plumes in the atmosphere.

The observational data and modeling results presented here demonstrate that extreme sulphate aerosol deposition can occur at a great distance from an eruption center. Understanding the geological causes, frequency, and atmospheric chemistry of these unfamiliar volcanic hazards, therefore, also bears important environmental and societal significance. In addition to volcanic eruptions, massive release of reduced sulphur gases can also be caused by bolide impacts or ocean overturning. Multiple isotope signatures of sulphate left behind by these dramatic geological events not only record the impacts on the atmosphere and surface conditions,

but also present new questions or hypotheses to be answered or tested in future observational as well as modeling studies. Sedimentary deposits in arid to semi-arid continental sites offer a rarely explored archive for such an effort.

Supplementary Information is linked to the online version of the paper at www.nature.com/nature.

References

[1] Wallace, P. J. Volcanic SO2 emissions and the abundance and distribution of exsolved gas in magma bodies. *Journal of Volcanology and Geothermal Research* **108**, 85-106 (2001).

[2] Self, S., Widdowson, M., Thordarson, T. & Jay, A. E. Volatile fluxes during flood basalt eruptions and potential effects on the global environment: A Deccan perspective. *Earth and Planetary Science Letters* **248**, 518-532, doi:10.1016/j.epsl.2006.05.041 (2006).

[3] Seinfeld, J. H. & Pandis, S. N. *Atmospheric Chemistry and Physics: From Air Pollution to Climate Change*. (Wiley, 1998).

[4] Robock, A. Perspectives: Pinatubo eruption: The climatic aftermath. *Science (Washington, DC, United States)* **295**, 1242-1244 (2002).

[5] National Atmospheric Deposition Program. 2008 Annual Summary. p. 15 (2009).

[6] Wignall, P. The link between large igneous province eruptions and mass extinctions. *Elements* **1**, 293-297 (2005).

[7] Ward, P. L. Sulfur dioxide initiates global climate change in four ways. *Thin Solid Films* **517**, 3188-3203, doi:10.1016/j.tsf.2009.01.005 (2009).

[8] Thordarson, T. & Self, S. Atmospheric and environmental effects of the 1783-1784 Laki eruption: A review and reassessment. *Journal of Geophysical Research-Atmospheres* **108** (2003).

[9] Mather, T. A. *et al.* Oxygen and sulfur isotopic composition of volcanic sulfate aerosol at the point of emission. *Journal of Geophysical Research-Atmospheres* **111**, doi:D18205 10.1029/2005jd006584 (2006).

[10] Rose, W. I. *et al.* Atmospheric chemistry of a 33-34 hour old volcanic cloud from Hekla Volcano (Iceland): Insights from direct sampling and the application of chemical box modeling. *Journal of Geophysical Research-Atmospheres* **111** (2006).

[11] Morin, S. *et al.* Tracing the Origin and Fate of NOx in the Arctic Atmosphere Using Stable Isotopes in Nitrate. *Science* **322**, 730-732, doi:10.1126/science.1161910 (2008).

[12] Bao, H. M. *et al.* Anomalous ^{17}O compositions in massive sulphate deposits on the Earth. *Nature* **406**, 176-178 (2000).

[13] Bao, H. M., Thiemens, M. H., Loope, D. B. & Yuan, X. L. Sulfate oxygen-17 anomaly in an Oligocene ash bed in mid-North America: Was it the dry fogs? *Geophysical Research Letters* **30**, 1843; 1810.1029/2003GL016869 (2003).

[14] Loope, D. B., Mason, J. A., Bao, H. M., Kettler, R. M. & Zanner, C. W. Deformation structures and an alteration zone linked to deposition of volcanogenic sulphate in an ancient playa (Oligocene of Nebraska, USA). *Sedimentology* **52**, 123-139 (2005).

[15] Bindeman, I. N., Eiler, J. M., Wing, B. A. & Farquhar, J. Rare sulfur and triple oxygen isotope geochemistry of volcanogenic sulfate aerosols. *Geochimica et Cosmochimica Acta* **71**, 2326-2343 (2007).

[16] Lyons, J. R. Transfer of mass-independent fractionation in ozone to other oxygen-containing radicals in the atmosphere. *Geophysical Research Letters* **28**, 3231-3234 (2001).

[17] Savarino, J., Bekki, S., Cole-Dai, J. & Thiemens, M. H. Evidence from sulfate mass independent oxygen isotopic compositions of dramatic changes in atmospheric oxidation following massive volcanic eruptions. *Journal of Geophysical Research [Atmospheres]* **108**, ACH 7/1-ACH 7/6 (2003).

[18] Noda, T. & Shimada, K. Water mixing model calculation for evaluation of deep geothermal water. *Geothermics* **22**, 165-180 (1993).

[19] Savarino, J., Lee, C. C. W. & Thiemens, M. H. Laboratory oxygen isotopic study of sulfur (IV) oxidation: Origin of the mass-independent oxygen isotopic anomaly in atmospheric sulfates and sulfate mineral deposits on Earth. *Journal of Geophysical Research -Atmospheres* **105**, 29079-29088 (2000).

[20] Savarino, J. & Thiemens, M. H. Analytical procedure to determine both $\delta^{18}O$ and $\delta^{17}O$ of H_2O_2 in natural water and first measurements. *Atmospheric Environment* **33**, 3683-3690 (1999).

[21] Johnston, J. C. & Thiemens, M. H. The isotopic composition of tropospheric ozone in three environments. *Journal of Geophysical Research [Atmospheres]* **102**, 25395-25404 (1997).

[22] Jenkins, K. A. & Bao, H. M. Multiple oxygen and sulfur isotope compositions of atmospheric sulfate in Baton Rouge, LA, USA. *Atmospheric Environment* **40**, 4528-4537 (2006).

[23] Bao, H. M. Sulfate in modern playa settings and in ash beds in hyperarid deserts: Implication on the origin of ^{17}O-anomalous sulfate in an Oligocene ash bed. *Chemical Geology* **214**, 127-134 (2005).

[24] Howell, K. J. & Bao, H. M. Caliche as a geological repository for atmospheric sulfate. *Geophysical Research Letters* **33** (2006).

[25] Alexander, B., Savarino, J., Barkov, N. I., Delmas, R. J. & Thiemens, M. H. Climate driven changes in the oxidation pathways of atmospheric sulfur. *Geophysical Research Letters* **29**, 1685, doi:10.1029/2002GL014879 (2002).

[26] Bao, H. M. & Marchant, D. R. Quantifying sulfate components and their variations in soils of the McMurdo Dry Valleys, Antarctica. *Journal of Geophysical Research-Atmospheres* **111**, DOI: 10.1029/2005JD006669 (2006).

[27] Armstrong, R. L. & Ward, P. L. Evolving geographic patterns of Cenozoic magmatism in the North American Cordillera; the temporal and spatial association of magmatism and metamorphic core complexes Mid-Tertiary Cordilleran magmatism; plate convergence versus intraplate processes. *Journal of Geophysical Research, B, Solid Earth and Planets* **96**, 13,201-213,224 (1991).

[28] Bao, H., Thiemens, M. H. & Heine, K. Oxygen-17 excesses of the Central Namib gypcretes: Spatial distribution. *Earth and Planetary Science Letters* **192**, 125-135 (2001).

[29] Eder, B. & Yu, S. C. A performance evaluation of the 2004 release of Models-3 CMAQ. *Atmospheric Environment* **40**, 4811-4824, doi:10.1016/j.atmosenv.2005.08.045 (2006).

[30] Zhang, D. D. *et al.* Precipitation chemistry of Lhasa and other remote towns, Tibet. *Atmospheric Environment* **37**, 231-240 (2003).

Acknowledgements

HB thanks Hannan LaGarry and James Swinehart for field guide, Margarita Khachaturyan, Kathryn Jenkins, Issaku Kohl, A. Jay Kaufman for technical assistance, and National Park Service for sampling permission at Scotts Bluff National Monument (permit# SCBL-2000-SCI-000, BADL-2004-SCI-0012, and SCBL-2004-SCI-0005). Financial support was provided by NSF (EAR-0408986 to HB). SY thanks Drs. S.T. Rao, D. Mobley, K. Schere, R. Mathur, J. Pleim, J. Godowitch, and S. Roselle for helpful comments. The United States Environmental Protection Agency through its Office of Research and Development funded and managed part of the research that is related to sulphur chemistry modeling. It has been subjected to Agency's administrative review and approved for publication. DT is grateful to Steve Fine, Daewon Byun, and Richard Artz for helpful discussion and acknowledges constructive internal ARL comments which have led to an improved manuscript.

Author Information

The authors declare no competing financial interests.

Correspondence and Requests for materials should be addressed to:

Huiming Bao (bao@lsu.edu), Shaocai Yu (yu.shaocai@epa.gov)

HB designed the research, did field and laboratory study, SY and DT did the 3-D sulphur oxidation and transport modeling study. HB wrote the manuscript. All authors contributed to manuscript revisions.

316 **Figure legends**

317 Fig. 1. Location of the northern High Plains, North America and a composite Eocene-
318 Oligocene-Miocene stratigraphy with seven ^{17}O-anomalous ($\Delta^{17}O > +1.4‰$) sulphate deposition
319 events recorded in tuffaceous beds. Solid bars indicate the relative positions of these ash beds.
320 See Supplementary Information for sources of the assigned numerical ages. CPF = Chamberlain
321 Pass Formation; PPM = Peanut Peak Member; BCCM = Big Cottonwood Creek Member; MC-H
322 FM = Monroe Creek-Harrison Formation. The two events in bold black, a 28 Myrs old and a 34
323 Myrs old, are the focus of this study. **(Brief title: Geological context of the samples)**

324

325 Fig. 2. Relationships between three sulphate stable isotope parameters, $\Delta^{17}O$, $\delta^{18}O$, and
326 $\delta^{34}S$, for sulphates extracted from the mid-Gering ash bed in Wildcat Ridge area, Nebraska
327 (upper panels) and J-ash at Pete Smith Hill, Nebraska (lower panels, except for one sample from
328 Alcova, Wyoming). There are two sets of sulphates: small blue diamonds for water extraction
329 and large red squares for HCl extraction. Error bars are equal to or smaller than symbols.
330 Superimposed triangles represent the end-member sulphate positions E1, E2, and E3 for the two
331 ash beds, respectively (Table S4). **(Brief title: Three sulphate end-member mixings)**

332

333 Fig. 3. Total column (0 to 2 km above the surface) sulphate flux (solid black) and $\Delta^{17}O$
334 value (dashed red) over time in western Nebraska, obtained from a 3-dimensional atmospheric
335 sulphur chemical-transport model, assuming 5 million-ton/day constant SO_2 emission rate from
336 an eruption in north-central Colorado, background cloudwater pH = 6 (upper), 7 (middle), and 8

(lower), and $[Fe^{2+}]$ and $[Mn^{2+}] = 10^{-5}$ μg/m^3. Left column is for winter and right for summer.

(<u>Brief title</u>: Modeling results on sulphate fluxes and $\Delta^{17}O$ values)

A potential eruption center at 28 Myrs ago

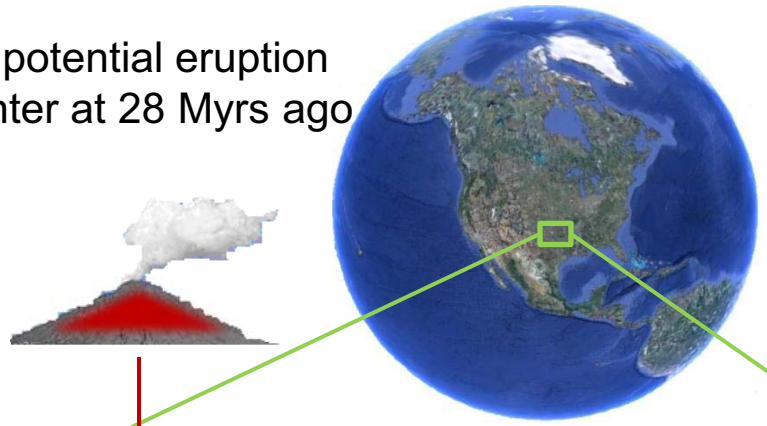

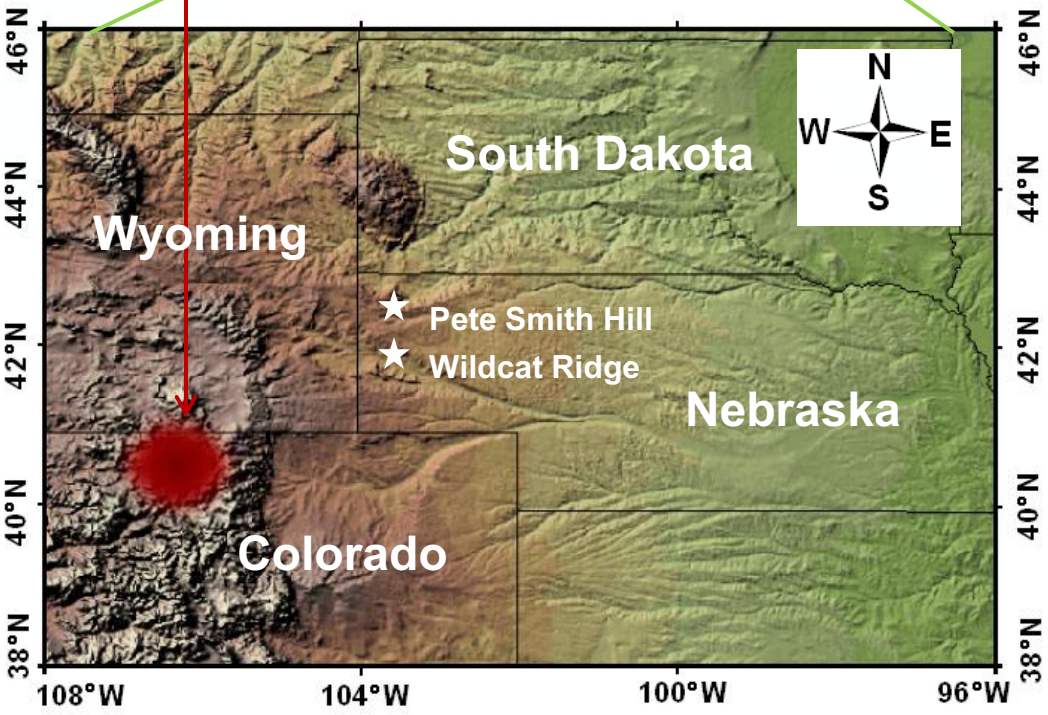

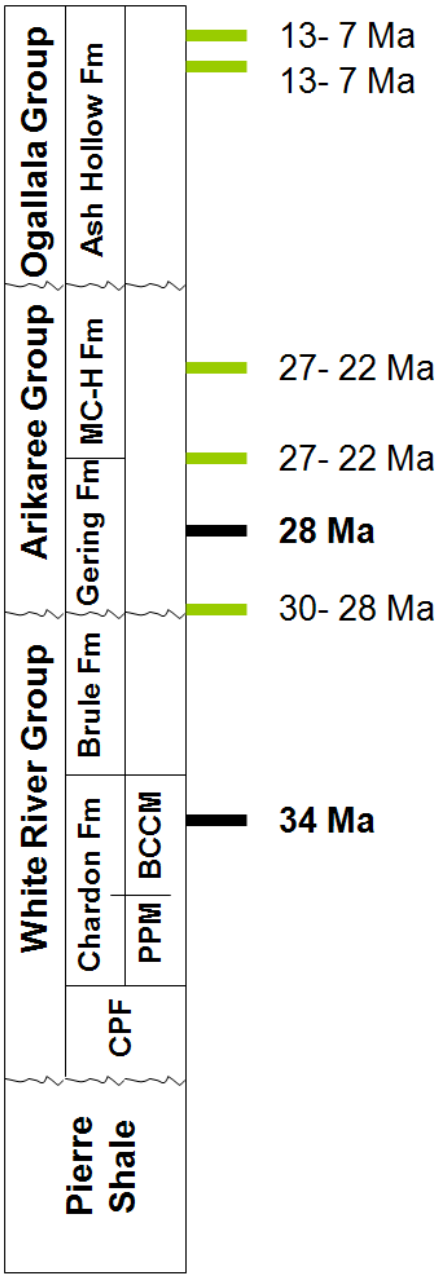

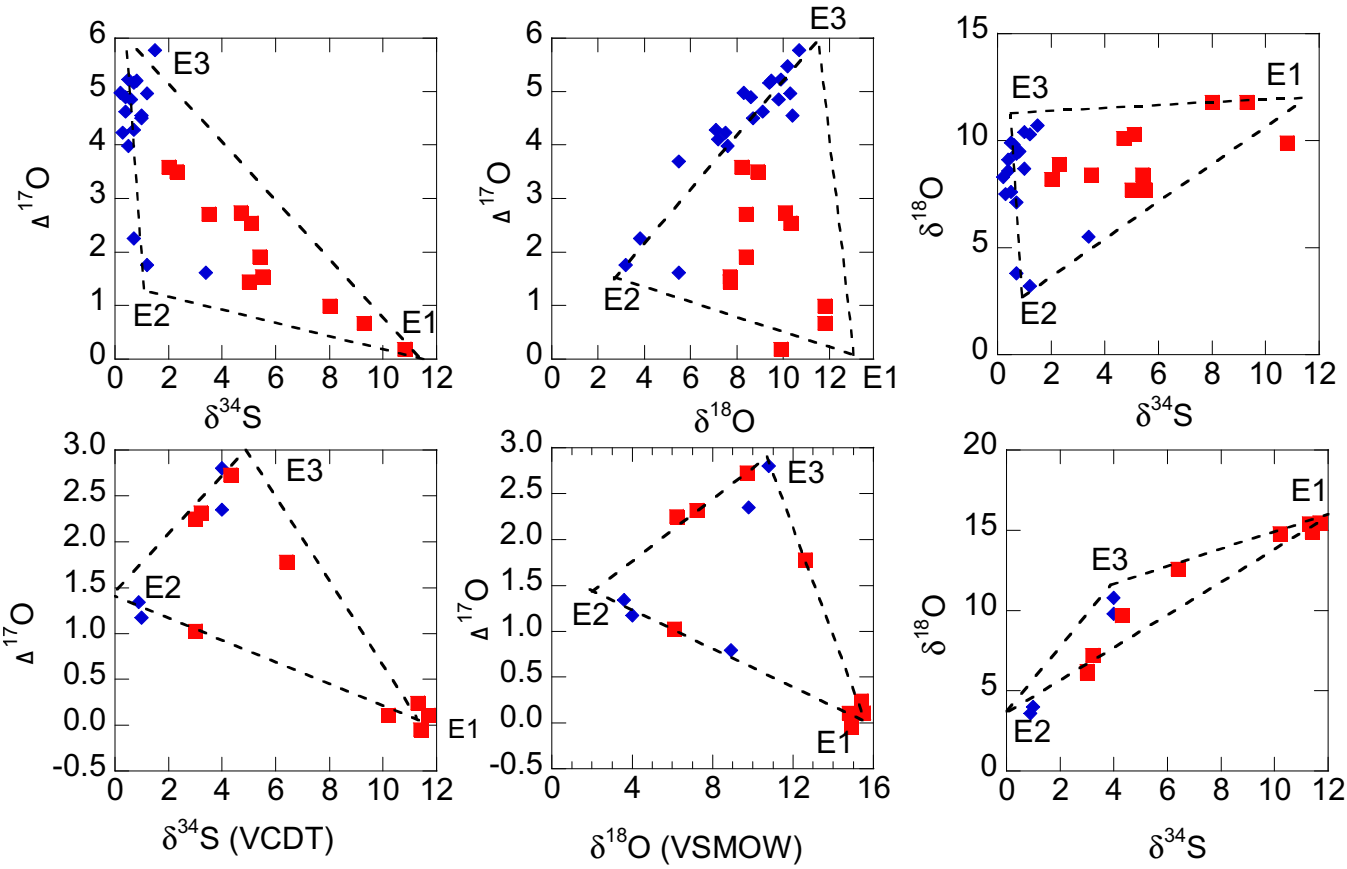
E3
E2
E1
Δ17O
δ34S
δ18O
δ34S (VCDT)
δ18O (VSMOW)

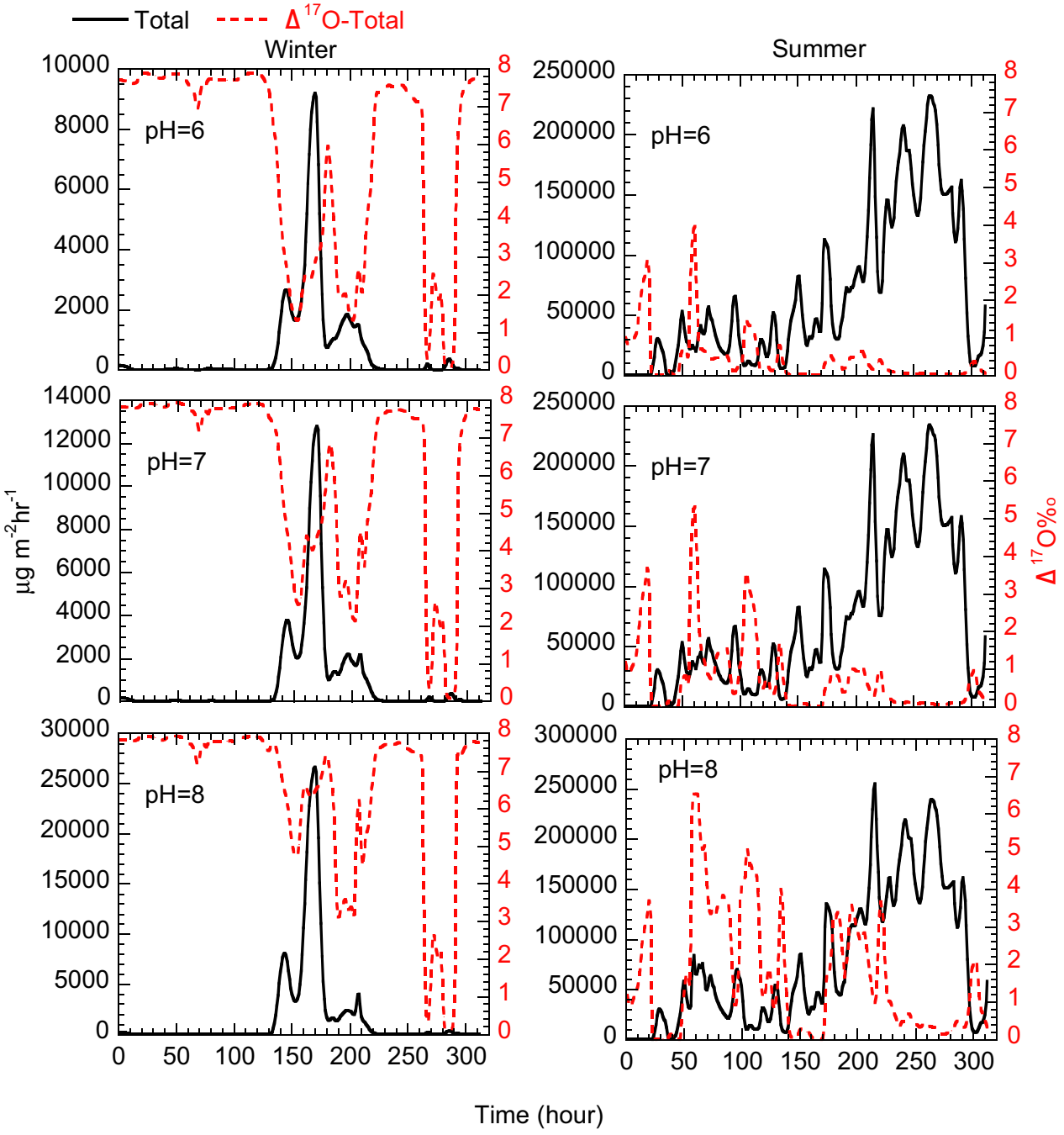
Total
Δ17O-Total
Winter
Summer
pH=6
pH=7
pH=8
μg m-2hr-1
Δ17O‰
Time (hour)

SUPPLEMENTARY INFORMATION

Massive volcanic SO_2 oxidation and sulphate aerosol deposition in Cenozoic North America

Huiming Bao[a], Shaocai Yu[b], and Daniel Q. Tong[c]

a. Department of Geology and Geophysics, Louisiana State University, Baton Rouge, LA 70803-4101 USA
b. Atmospheric Modeling and Analysis Division, National Exposure Research Laboratory U.S. Environmental Protection Agency RTP, NC 27711 USA
c. Air Resources Laboratory, National Oceanic and Atmospheric Administration, Silver Spring, MD 20910, USA

Table S1. Composite column for Cenozoic ash beds that bear sulphate $\Delta^{17}O \geq +1.4‰$

Sample	$\Delta^{17}O$	Age (Ma)	Formation	Location	Note
LB-42	1.75	13 to 7 [1]	The Ash Hollow Formation, Ogallala Group	Broadwater, Nebraska (NE)	Ogallala ash bed 3
LB-40	1.39	13 to 7 [1]	The Ash Hollow Formation, Ogallala Group	Broadwater, NE	Ogallala ash bed 4
LB-13	2.17	27 to 22 [2]	At the base of Monroe Creek-Harrison Formation, Arikaree Group	Scotts Bluff National Monument (SBNM), NE	
LB-30	1.42			Chimney Rock National Monument, NE	
LB-17	5.05	27 to 22 [2]	At the lower part of the Monroe Creek-Harrison Formation, Arikaree Group	SBNM, NE	
LB-32	1.14				
B00-11, 12	2.21* 2.78*	~ 28 (via stratigraphic correlation)	At the upper part of the Sharps Formation, Arikaree Group	Saddle Pass Trail, Notch Trail, Badlands Nation Park (BNP)	
B00-24, -25					
LB-5, -6	5.77*	~ 28 [2]	At the middle of the Gering Formation, Arikaree Group	SBNM, NE	The mid-Gering ash bed [3]
LB-36	2.64			Hawking Springs, Wyoming	
LB-3A	5.27	28 to 30 #[4]	At the base of the Gering Formation, Arikaree Group	SBNM, Gering, NE	
B00-34	1.12	~ 30 [5]	The Sharps Formation, Arikaree Group	Notch Trail, BNP, South Dakota (SD)	Rockyford Ash
B00-16	1.93			Saddle Pass Trail, BNP, SD	
G3-2	2.32	34.36 [6]	The Big Cottonwood Creek member, Chardon Formation, White River Group	Pete Smith Hill, Crawford, NE	J ash, correlated by E.E. Larson [7]
WPT212	2.80				
WPT219	2.73			Alcova, Wyoming	

* The highest value is shown here for multiple samples from the same bed.
# The base of the Gering Formation in northwestern Nebraska is probably equivalent to the Rockyford Ash bed in South Dakota, on the basis of the $\Delta^{17}O$ sequences from the two basins.

Table S2. The $\delta^{18}O$ (VSMOW), $\Delta^{17}O$, and $\delta^{34}S$ (VCDT) values (all new data) for sulphates extracted from the mid-Gering ash bed (The Gering Formation, Arikaree group) in the Wildcat Ridge area (~41°25' to 42°05'N; ~102°50' to 104°00'W), Western Nebraska, U. S. A.

Samples	$\delta^{18}O$	$\Delta^{17}O$	$\delta^{34}S$
Water extraction			
LB-5-a	9.5	5.20	0.8
LB-5-b	9.8	4.85	0.6
LB-5-e	8.7	4.50	1.0
LB-5-f	8.6	4.89	0.4
LB-6(1)-a	5.5	3.69	-0.4
LB-6(1)-b	3.8	2.26	0.7
LB-6(1)-c	3.2	1.76	1.2
LB-6(2)-a	7.1	4.28	0.7
LB-6(2)-b	7.2	4.11	
LB-6(2)-c	7.6	3.98	0.5
LB-6(2)-d	7.5	4.23	0.3
LB-6(3)-a-no-0.2um	9.9	5.23	0.5
LB-6(3)-b	10.7	5.77	1.5
LB-6(3)-c	10.2	5.47	-0.1
LB-6(3)-d	8.3	4.98	0.2
LB-6(3)-e	9.4	5.16	0.7
Drp-WR169-1-1	10.4	4.55	1.0
Drp-WR169-1-2	5.5	1.61	3.4
Drp-WR158-1-1	9.1	4.62	0.4
Drp-WR158-1-2	10.3	4.97	1.2
HCl-extraction			
LB-6(1)-1-AE	7.7	1.54	5.5
LB-6(1)-2-AE	8.4	1.92	5.4
LB-6(1)-3-AE	7.7	1.45	5.0
LB-6(2)-a-AE	8.4	2.71	3.5
LB-6(2)-b-AE	8.2	3.59	2.0
LB-6(2)-c-AE	8.9	3.51	2.3
LB-6(2)-d-AE	10.1	2.74	4.7
Drp-WR169-1-1-AE	10.3	2.55	5.1
Drp-WR169-1-2-AE	9.9	0.19	10.8
Drp-WR158-1-1-AE	11.8	0.99	8
Drp-WR158-1-2-AE	11.8	0.67	9.3

Table S3. The $\delta^{18}O$, $\Delta^{17}O$, and $\delta^{34}S$ values for sulphates extracted from the "J" ash bed (in the Chadron Formation, White River group) in the Pete Smith Hill area, northwestern Nebraska (42°55'N; 103°27'W), and one sample (WPT219, 42°32.6'N;106°49.7'W) from "J" ash at Alcova, WY, U. S. A.

Sample	$\delta^{18}O$	$\Delta^{17}O$	$\delta^{34}S$
Water extraction			
WPT212B-W	4.0	1.17	1.0
WPT212B-W-2	3.6	1.34	0.9
WPT217B(1)-W	10.8	2.80	4.0
WPT217B(1)-W-2	9.8	2.35	4.0
WPT217B(2)-W	8.9	0.79	n. a.*
HCl-extraction			
G3-2-KH-repro	7.2	2.32	3.2
G3-2-F	6.2	2.25	3.0
WPT212B	6.1	1.03	3.0
WPT213B	14.9	-0.05	11.4
WPT214B	14.8	0.11	10.2
WPT216B(1)	15.4	0.24	11.3
WPT216B(2)	15.5	0.11	11.7
WPT217B(1)	12.6	1.78	6.4
WPT219	9.7	2.73	4.3

* Not available due to small sample size.

Table S4. End-member oxygen and sulphur isotope composition for sulphate in two volcanic ash beds, Cenozoic North America, determined by self-consistent Weighted Least Squares (WLS) method without any prior assumption of the number or composition of the end-members.

	$\delta^{18}O$	$\Delta^{17}O$	$\delta^{34}S$
Wildcat Ridge, NE, ~28 Ma			
end-member-1	12.7	0.0	11.7
end-member-2	2.5	1.5	1.0
end-member-3	11.2	6.0	0.3
Pete Smith Hill, NE, ~34 Ma			
end-member 1	15.7	0.0	11.6
end-member 2	2.3	1.4	0.0
end-member 3	10.5	2.9	4.4

Summary of laboratory methods

Differing from previous study[3] in which only water-soluble sulphate was measured, this paper reports the $\delta^{18}O$, $\Delta^{17}O$, and $\delta^{34}S$ of sulphate extracted by water and/or by acid (HCl) on the same rock sample. In addition, all barite ($BaSO_4$) precipitates were treated twice with DDARP method[8] to ensure barite is free of nitrate and other contaminants. Well-cemented tuffaceous beds were collected from the field and were cleaned off the surface and grinded to fines using mortar and pestle in the laboratory. Sulphate was first extracted using doubly-deionized H_2O and then separately using a 1 M HCl solution. These sulphate fractions were precipitated as $BaSO_4$. The $BaSO_4$ was subsequently purified using the DDARP method[8] in which the barite was dissolved using DTPA (a chelating agent) and re-precipitated by acidification using 10M HCl droplets. O_2 was extracted using a CO_2-laser fluorination system[9] and measured for both $\delta^{17}O$ and $\delta^{18}O$ values simultaneously on a Finnigan MAT 253 in a dual-inlet mode. The average O_2 sample size is ~ 25 micro-moles, and is ~ 25% to 35% of the total barite oxygen yield. The standard deviation associated with the $\Delta^{17}O$ is ± 0.03‰ for multiple (N ~3) runs of the same O_2 gas on the MAT 253, and ±0.05‰ for replicates of the same $BaSO_4$ via CO_2-laser fluorination. The $\delta^{17}O$ value was initially calibrated against UWG-2, assuming its $\delta^{18}O$ = +5.80‰ (VSMOW)[10] and its $\delta^{17}O$ = 3.016‰ (0.520 × $\delta^{18}O$). The reported $\delta^{18}O$ was measured using a Temperature Conversion Elemental Analyzer (TCEA) (reactor temperature at 1450°C) coupled to a MAT 253 in a continuous-flow mode**.** Stable isotope measurements at LSU OASIC are run above certain threshold of gas pressure (~ 20-25 mbar) and are based on an extrapolation of the VSMOW (i.e. UWG-2) measurements,

assuming ideal linear mass-spectrometric performance (single reference approach). The $\delta^{34}S$ was measured using an EA (reactor temperature at 1050°C) coupled to a Micromass Isoprime at A. J. Kaufman's laboratory at University of Maryland.

The $\delta^{18}O$ and $\delta^{34}S$ have standard deviations of 0.5‰ and 0.3‰, respectively, and their values were calibrated against NBS127 with an assigned values of +9.3‰ (VSMOW) and +21.1‰ (VCDT), respectively. Except for the $\delta^{34}S$ analysis, all other experiments were conducted at Oxy-Anion Stable Isotope Center (OASIC) at Louisiana State University.

Description of the self-consistent weighted Least Squares method for end-member characterization

An established approach to characterize chemical and/or isotopic end-members in a conservative mixing system, without any prior assumption of the number or composition of the end members, is the self-consistent Weighted Least Squares (WLS) method[11,12,13,14]. Sulphate in this study was likely quickly deposited and cemented in arid to semi-arid continental environments, thus meeting the condition of a conservative mixing. The WLS method produced a three end-member-mixing scenario for both the Wildcat Ridge and the Pete Smith Hill datasets. This statistical treatment was assisted by Prof. Bin Li at the Department of Statistics at LSU.

The algorithm of our WLS method

Notation

N: number of samples
M: number of isotopic components
L: number of source sulphate
R: N × L mixing matrix (mixing fractions of source sulphate)
S: L ×M source (end-member) matrix (values of the isotope components in source)
D: N×M sample matrix (values of the isotope components in collected samples)

Model

$\boldsymbol{D = R \times S}$

Constrains for mixing matrix ***R***:

(1) all elements are non-negative,
(2) each row sums up to one.

Algorithm

Step 1: Initialization.

(1) Initialize the source (end-member) matrix ***S***.
(2) The eye-balled estimate is used as our initial estimate of ***S***.
(3) Set the weight for each isotope component ($\delta^{34}S$:$\delta^{18}O$:$\Delta^{17}O$ =1:1:10 based on analytical accuracy).

(4) Set $j \leftarrow 1$.

Step 2: Estimate the mixing matrix $\boldsymbol{R}$ given $\boldsymbol{S}$ and $\boldsymbol{D}$.

(1) The estimation of $\boldsymbol{R}$ is based on constrained weighted least-square method. It involves two constrains.
   (a) Equality constraint - the row sum of $\boldsymbol{R}$ is one.
   (b) Inequality constraint – all elements are non-negative.
(2) Note: each row of $\boldsymbol{R}$ is estimated separately.

Step 3: Calculate the estimation error.

(1) Update: $\boldsymbol{D_j} = \boldsymbol{R} \times \boldsymbol{S}$
(2) $E_j = \sum |(\boldsymbol{D} - \boldsymbol{D_j})/\boldsymbol{D_j}|$ (summation and subtraction are both taken element-wise).
(3) $j \leftarrow j + 1$

Step 4: Estimate the end-member matrix $\boldsymbol{S}$ given $\boldsymbol{R}$ and $\boldsymbol{D}$.

Each column (component) of $\boldsymbol{S}$ is estimated through weighted least-square method separately.

Update: $\boldsymbol{D_j} = \boldsymbol{R} \times \boldsymbol{S}$ and $j \leftarrow j + 1$

Step 5: Calculate the estimation error.

(1) Update: $\boldsymbol{D_j} = \boldsymbol{R} \times \boldsymbol{S}$
(2) $E_j = \sum |(\boldsymbol{D} - \boldsymbol{D_j})/\boldsymbol{D_j}|$ (summation and subtraction are both taken element-wise).
(3) $j \leftarrow j + 1$

Step 6: Check stopping criterion.

Stop if E_j either converges or reaches the minimum value, otherwise repeat Step 2 – Step 5.

The algorithm is based on Noda and Shimada (1993)[12] and Van Geen and Boyle (1990)[14].

Description of a 3-dimensional atmospheric chemical transport model (CMAQ) and model simulations

The latitude position, global ocean/atmospheric condition, and landscape of North America continent in ~28 Myrs ago were generally similar to those of today. For our purpose (i.e. to see if a simulated SO_2 plume can generate the sulphate isotope signatures observed in rock record), the important difference is that today the atmospheric sulphur budget is overwhelmed by anthropogenic inputs. Therefore, our model looks at a preindustrial atmosphere over the continental U.S. simulated by the U.S. EPA Models-3/Community Multiscale Air Quality (CMAQ) model[15] with the Sulphate Tracking Model option[16]. Modeling domain spans the continental United States with 36-km horizontal grids (see Fig. S1). Fourteen layers of variable thickness are specified on a hybrid sigma pressure vertical coordinate system to resolve the atmosphere between the surface and 100 hPa (~13.6 km). The thickness of surface layer is about 38 m, and layer 9 is ~ 2 km above the surface. Meteorological inputs for the CMAQ model are obtained from the MM5 mesoscale model using the configuration described by Eder and Yu[17]. The preindustrial emissions include wildfires, biogenic emissions (soil, grassland and forest), and natural dust emissions. Emissions of human origins, such as cars, power plants, residential area, aircraft, trains, and marine vehicles are excluded in our model simulations.

The CMAQ sulphate tracking model can track sulphate chemical productions from gas-phase ·OH oxidation and five aqueous-phase chemical reactions which include aqueous-phase S (IV) oxidation reactions by H_2O_2, O_3, oxygen catalyzed by Fe^{3+} and

Mn^{2+}, methyle hydrogen peroxide and peroxyacetic acid (Table S5). The clean lateral boundary conditions for the model simulations were provided by the global Model of Ozone and Related Chemical Tracers, Version 2 (MOZART-2)[18]. In the MOZART-2 global simulation, surface emissions of chemical species include those from biomass burning, biogenic emissions from vegetation and soils, and oceanic emissions, and are intended to be representative of emissions in the early 1870s[18].

The Carbon Bond chemical mechanism (CB05)[19] has been used to represent photochemical reaction pathways in CMAQ. The aerosol module in CMAQ is described by Binkowski et al[20] and updates are described by Bhave et al[21] and Yu et al[22]. In the aerosol module of the CMAQ, the aerosol distribution is modeled as a superposition of three lognormal modes that correspond nominally to the ultrafine (diameter (Dp) < 0.1 mm), fine (0.1 < Dp < 2.5 mm), and coarse (Dp > 2.5 mm) particle sizes. Each lognormal mode is characterized by total number concentration, geometric mean diameter and geometric standard deviation. The model results for $PM_{2.5}$ concentrations are obtained by summing aerosol species concentrations over the first two modes. A model spin-up period of 3 days was used to mitigate the effects of initial conditions on the model results. In this study, the hourly model results within planetary boundary layer (PBL) between the surface and a height of ~2 km (corresponding to layer 9 in this model) from June 18 to 30, 2002 (summer case) and December 18 to 30, 2002 (winter case) are used, except the case for stratospheric O_3 input in which we summarize all 1 to 14 layers. Since during the daytime SO_2 and sulphate are well mixed vertically through the PBL, we choose 2 km[23] as being representative of the mean daytime PBL height for this analysis.

To simulate the impact of volcanic SO_2 ejection on the troposphere, we have run model simulations with various combinations of variables, including SO_2 emission rate (5000-ton to 5-million-ton/day, see Figure S3), emission type (point source or dispersed over a column, see Figure S3), meteorology (summer and winter, see Figures S2, and S6), dissolved $[Fe^{2+}]$ or $[Mn^{2+}]$ content (e.g. 10^{-10}, 10^{-5}, and 10^{-2} μg/m^3, see Figures S4 and S5), initial cloudwater pH (4, 6, 7, 8, and 9 set by background Ca^{2+} concentrations, see Figure 3), and stratospheric input of O_3 via tropopause folding (Figure S6). In the case of emissions, a fixed, continuous flux of SO_2 emission was released as a point source at around 2 km or dispersed between 3 km and 8 km above a volcanic site at 40°50′N 106°16′W (north central Colorado) (Figures S1 and S3). As shown in Figure S3, when all other variables are fixed, higher SO_2 emission rate will reduce the magnitude of $\Delta^{17}O$ of the total sulphate, and the difference for the magnitudes of $\Delta^{17}O$ for total sulphate between point and column sources is very small in the case of 5-million-ton/day emission although the total sulphate flux is slightly higher for the point source case.

In the CMAQ model, the default values for dissolved $[Fe^{2+}]$ and $[Mn^{2+}]$ concentrations are 10^{-2} μg/m^3 and 5×10^{-3} μg/m^3, respectively. We think these parameters, which are based on modern atmosphere averages, are too high for an Oligocene (28 million years ago) atmosphere. Considering that metal content of the atmosphere may increase during a volcanic eruption, we adopted the lower limit of dissolved $[Fe^{2+}]$ and $[Mn^{2+}]$ in modern atmosphere used by Alexander et al[24]; we use 10^{-5} μg/m^3 for both dissolved $[Fe^{2+}]$ and $[Mn^{2+}]$. Increasing the content of $[Fe^{2+}]$ and $[Mn^{2+}]$ will lower the $\Delta^{17}O$ of total sulphate flux. However, the $\Delta^{17}O$ of total sulphate flux remains low even when $[Fe^{2+}]$ and $[Mn^{2+}]$ are set to = 10^{-10} μg/m^3 if the background atmosphere is acidic to

begin with (Figure S4). In other conditions, there are no differences in results when the $[Fe^{2+}]$ and $[Mn^{2+}]$ are below certain level (e.g. Figure S5).

Since the default value of dissolved Ca^{2+} is zero in the CMAQ mode, the default values of cloudwater pH for the atmosphere under our conditions are around 4 (acidic). According to 15-year continuous measurements obtained from a National Acidic Deposition Assessment Network in Nebraska (site NE99), the weekly pH values in rainwater range from 4.3 to 7.5 (figure S7) in western Nebraska, however. On days with high dust emissions, indicated by high concentrations of calcium, a fingerprint of mineral dust, the pH values are generally high (Figure S7). As an example, Figure S8 shows the temporal variations of concurrent and dramatic changes of pH and $[Ca^{2+}]$ at this site. Our study indicates that the puzzling sulphate isotope pattern can be realized only when the initial atmosphere pH value for cloud water in the northern High Plains of North America was alkaline during the mid-Cenozoic (see Figure 3). This is also consistent with the results of Seinfeld and Pandis[25] who find that at pH values less than roughly 4 to 5, the predominant pathway for sulphate formation is oxidation of SO_2 by dissolved H_2O_2, and at pH $\geq$ 5 oxidation by O_3 starts to dominate and at pH = 6 it is 10 times faster than that by H_2O_2. To examine the background cloudwater pH effect, we have run model simulations with different background cloudwater pH (4, 6, 7, 8, and 9) set by background Ca^{2+} concentrations (see Figure 3).

To study possible effect of tropopause folding events that add stratospheric O_3 into the upper troposphere, we have run model simulations in which all O_3 concentrations are maintained at 120 ppbv above 4 km (Layer 11 to 14 in the model). The stratospheric

O_3 addition does increase total sulphate flux, but only adds a little to the total sulphate $\Delta^{17}O$ value for both winter and summer cases (see Figure S6).

The CMAQ model is developed and tested based largely on modern atmospheric / meteorological conditions and our current scientific knowledge of aqueous- and gas-phase sulphur oxidation chemistry in the atmosphere. Despite an effort to use preindustrial background sulphur emission in our modeling experiments, when applied to massive volcanic SO_2 emission events in continental interior of an Oligocene Earth, the model has two potential caveats: 1) a lack of atmospheric chemistry-meteorology feedback (e.g. massive SO_2 oxidation may alter meteorological conditions in a significant way); and 2) the unknown roles played by dusts associated with volcanic eruptions. However, importantly, these model deficiencies are not going to affect the core interpretation of our modeling results because variations in the concentrations of O_3, cloud-pH value, and meteorological conditions (summer and winter) resulting from these possible caveats have been considered in our sensitivity tests as described previously.

Table S5. List of sulphate species from various chemical oxidation pathways

Species name	**Description**
ASO4AQH2O2J	ASO4J produced by aqueous-phase hydrogen peroxide oxidation reaction: H_2O_2 + S(IV) -> S(VI) + H_2O
ASO4AQO3J	ASO4J produced by aqueous-phase ozone oxidation reaction: O_3 + S(IV) -> S(VI) + O_2
ASO4AQFEMNJ	ASO4J produced by aqueous-phase oxygen catalyzed by Fe+++ and Mn++ oxidation reaction: O_2 + S(IV) -> S(VI)
ASO4AQMHPJ	ASO4J produced by aqueous-phase methyl hydrogen

	peroxide oxidation reaction: MHP + S(IV) -> S(VI)
ASO4AQPAAJ	ASO4J produced by aqueous-phase peroxyacetic acid oxidation reaction: PAA + S(IV) -> S(VI)
ASO4GASI	ASO4I nucleated and/or condensed following gas-phase reaction: $\cdot OH + SO_2$ -> SULF + $\cdot HO_2$
ASO4GASJ	ASO4J nucleated and/or condensed following gas-phase reaction: $\cdot OH + SO_2$ -> SULF + $\cdot HO_2$

* I and J represent nucleation and fine modes, respectively. The results are displayed the sum of both.

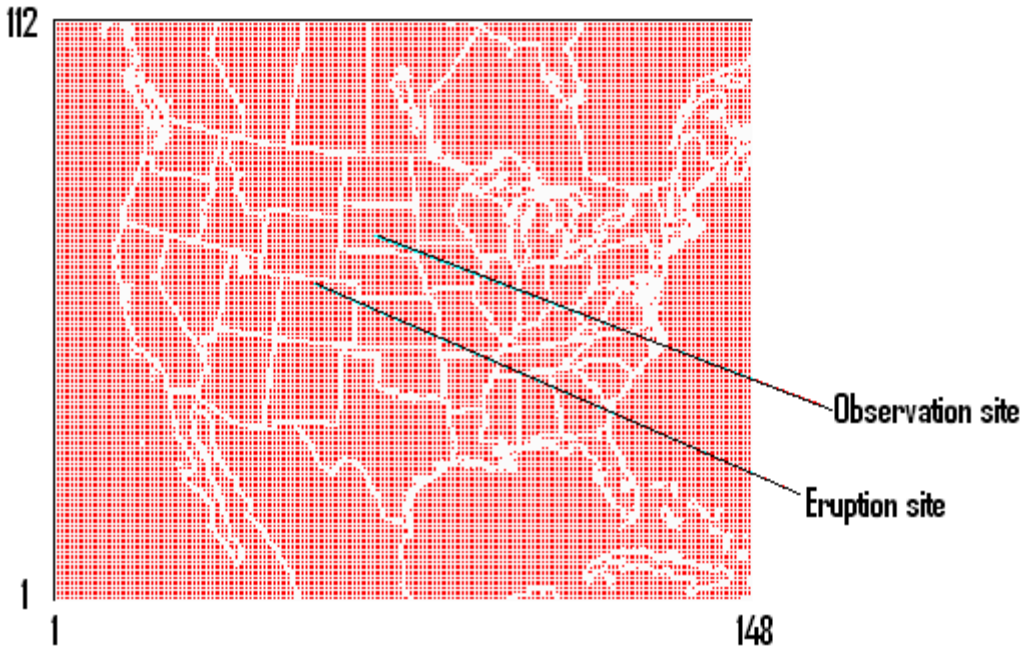

Fig. S1. The model domain and locations of volcano eruption site (north-central Colorado) and observation site (western Nebraska, U. S. A.).

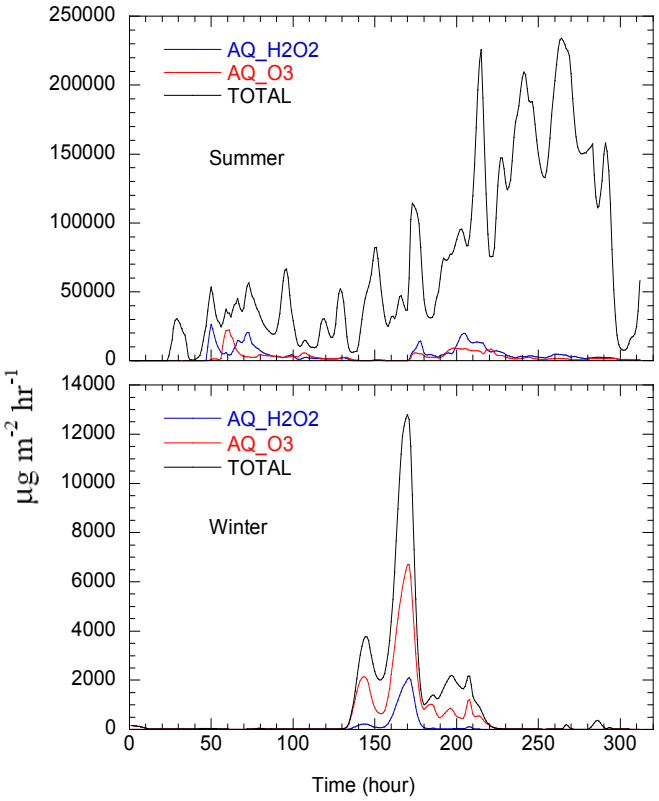

Fig. S2. Sulphate flux over time in western Nebraska after an eruption in north-central Colorado; assuming 5 million-ton/day constant SO_2 emission rate and a summer (upper) vs. winter (lower) meteorological condition. Background cloudwater pH=7, $[Fe^{2+}] = 10^{-5}$ $\mu g/m^3$.

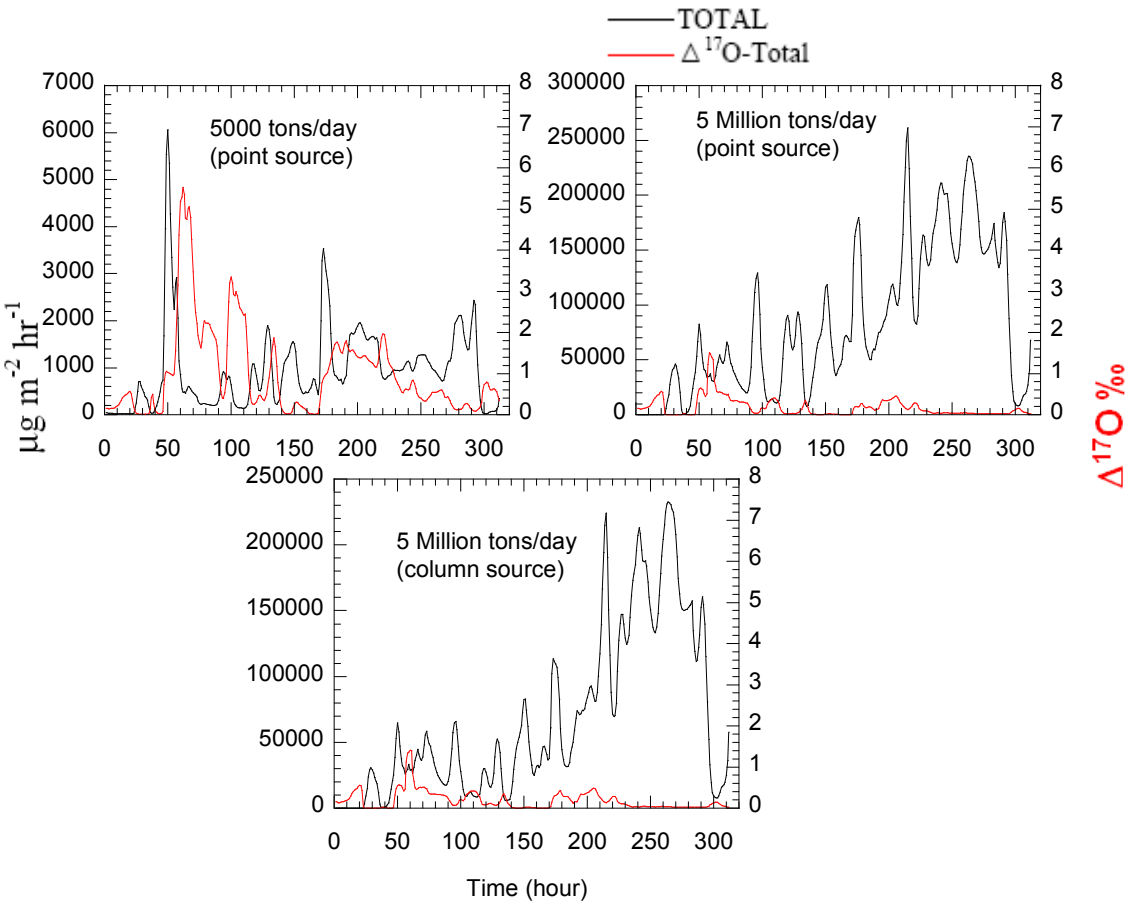

Fig. S3. Total sulphate flux and $\Delta^{17}O$ value over time in western Nebraska after an eruption in north-central Colorado; assuming 5000 tons/day (upper left) and 5 million-ton/day (upper right and lower), constant SO_2 emission rate, and a summer meteorological condition. "Point source" means release of the SO_2 source at around 2 km above the ground and "column source" means release of the SO_2 source between 3 km and 8 km above the ground. A CMAQ model with preindustrial sulphur emission is used (e.g. Background cloudwater pH= 4, $[Fe^{2+}] = 10^{-2}$ μg/m^3).

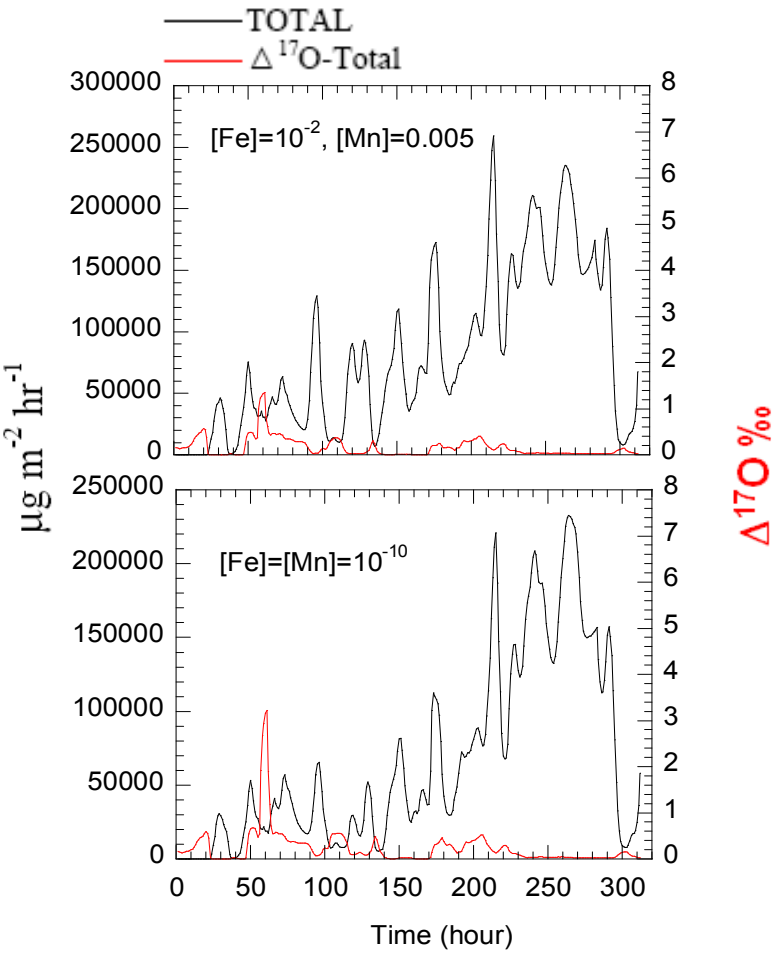

Fig. S4. Total sulphate flux and $\Delta^{17}O$ value over time in western Nebraska after an eruption in north-central Colorado; assuming 5 million-ton/day, constant SO_2 emission rate, and a summer meteorological condition. A CMAQ model with preindustrial sulphur emission is used: background cloudwater pH= 4, $[Fe^{2+}] = 10^{-2}$ and $[Mn^{2+}] = 5\times10^{-3}$ $\mu g/m^3$ (upper) and $[Fe^{2+}] = [Mn^{2+}] = 10^{-10}$ $\mu g/m^3$ (lower).

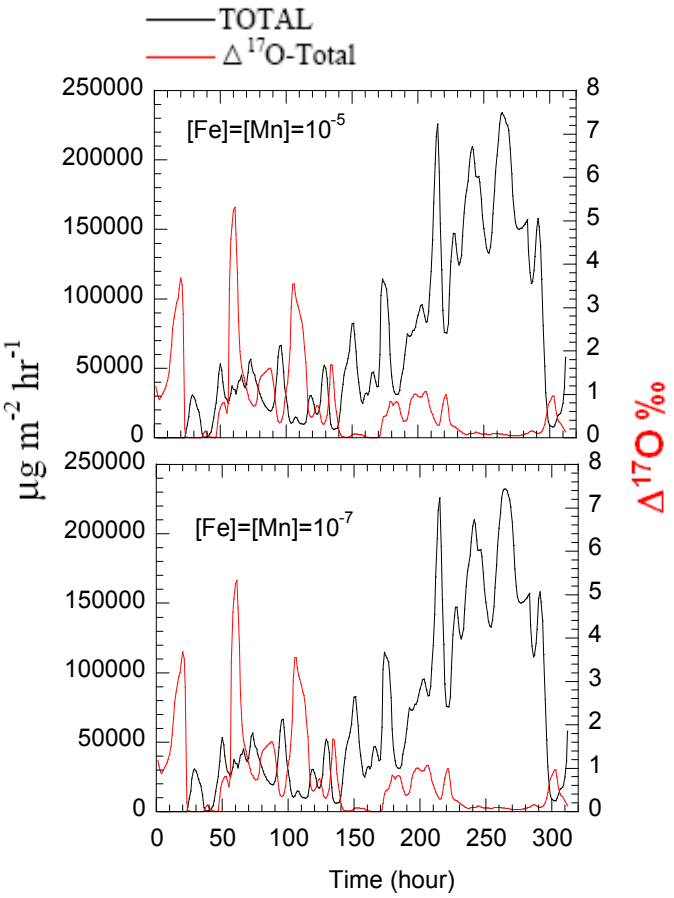

Fig. S5. Total sulphate flux and $\Delta^{17}O$ value over time in western Nebraska after an eruption in north-central Colorado; assuming 5 million-ton/day, constant SO_2 emission rate, and a summer meteorological condition. A CMAQ model with preindustrial sulphur emission is used: background cloudwater pH= 7, $[Fe^{2+}] = [Mn^{2+}] = 10^{-5}$ μg/m^3 (upper) and $[Fe^{2+}] = [Mn^{2+}] = 10^{-7}$ μg/m^3 (lower). There is essentially no difference in results between these two different Fe^{2+} & Mn^{2+} concentration levels.

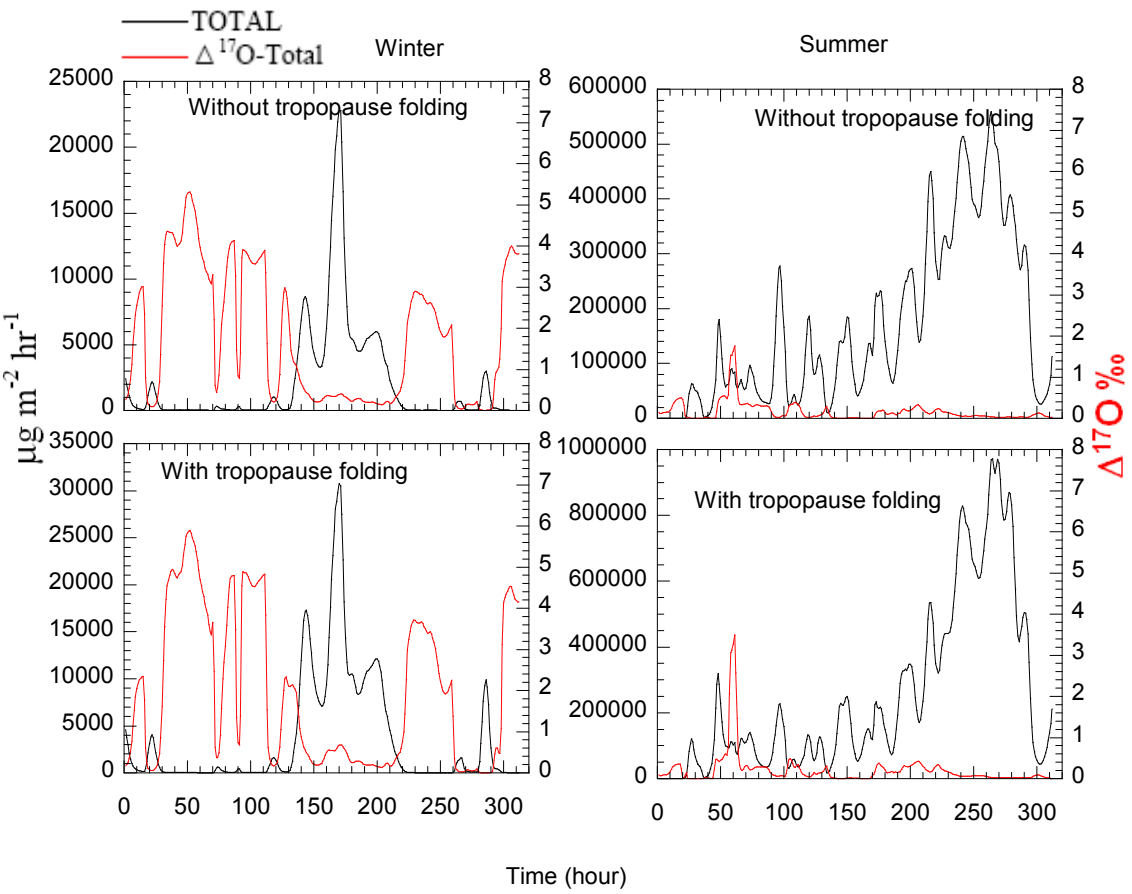

Fig. S6. Total sulphate flux (Layer 1 to 14) and $\Delta^{17}O$ value over time in western Nebraska after an eruption in north-central Colorado; assuming 5 million-ton/day, constant SO_2 emission rate, and winter and summer conditions. A CMAQ model with preindustrial sulphur emission is used: background cloudwater pH= 4, $[Fe^{2+}] = 10^{-2}$ and $[Mn^{2+}] = 5\times10^{-3}$ μg/m^3 (upper one). The lower one shows a case of stratospheric input of O_3 via tropopause folding, in which all O_3 concentrations are set to be 120 ppbv above 4 km (Layer 11 to 14 in the model). The stratospheric input does increase total sulphate flux, but only a little to the total sulphate $\Delta^{17}O$ value. Left column is for winter and right for summer

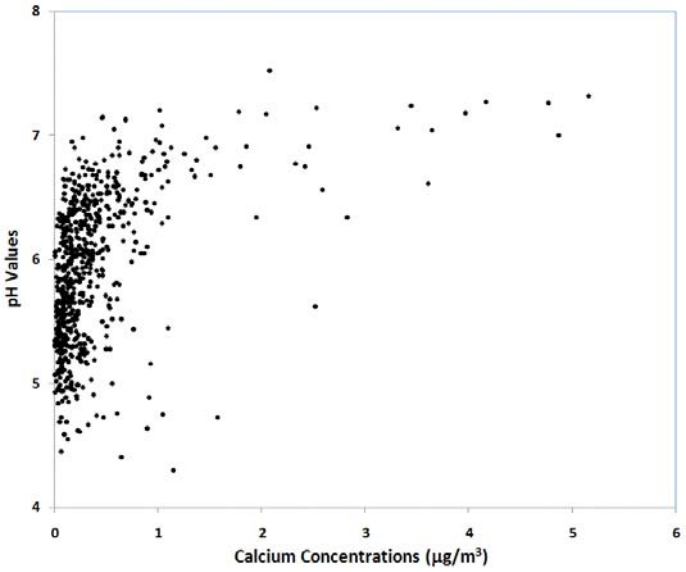

Fig. S7. Correlation between pH values and Calcium concentrations in rainwater observed at the Nebraska NADP site (NE99) from 1985 to 2009. The data shows when the concentration of Calcium, an elemental abundant in mineral dust, is lower than 3.0 µg/m^3, the rainwater has a wide range of alkalinity, with pH values ranging from 4.3 to 7.5. When the Calcium concentration is above 3.0 µg/m^3, usually indicting the effect of mineral dust emissions, the rainwater pH values are constantly high.

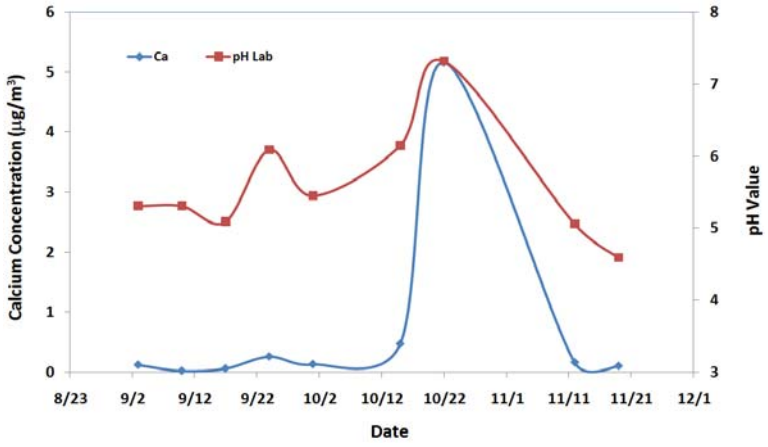

Fig. S8. Time series of weekly pH values and calcium concentrations measured at the NADP site (NE99) from September to November 1996. Rainwater pH values increase exponentially with calcium peaks

References

1 Perkins, M. E., Diffendal, R. F. J. & Voorhies, M. R. in *Geological Society of America, 29th annual meeting, North-Central Section, South-Central Section* Vol. 27, 79 (Geological Society of America (GSA), 1995).

2 MacFadden, B. J. & Hunt, R. M., Jr. in *Depositional environments, lithostratigraphy, and biostratigraphy of the White River and Arikaree groups* Vol. 325 *Special Paper - Geological Society of America* eds Dennis O. Terry, Hannan E. LaGarry, & Robert M. Jr. Hunt) 143-165 (Geological Society of America -- Special Paper, 1998).

3 Bao, H. M., Thiemens, M. H., Loope, D. B. & Yuan, X. L. Sulfate oxygen-17 anomaly in an Oligocene ash bed in mid-North America: Was it the dry fogs? *Geophysical Research Letters* 30, 1843; 1810.1029/2003GL016869 (2003).

4 Swisher, C. C., III & Prothero, D. R. Single-crystal $^{40}Ar/^{39}Ar$ dating of the Eocene-Oligocene transition in North America. *Science* 249, 760-762 (1990).

5 Prothero, D. R. & Swisher, C. C. I. in *Eocene-Oligocene climatic and biotic evolution* eds D. R. Prothero & W. A. Berggren) 46-73 (Princeton University Press, 1992).

6 Obradovich, J. D., Evanoff, E. & Larson, E. E. Revised single-crystal laser-fusion $^{40}Ar/^{39}Ar$ ages of Chadronian tuffs in the White River Formation of Wyoming. *Geological Society of America, 29th annual meeting, North-Central Section, South-Central Section* 27, 77-78 (1995).

7 Terry, D. O., Jr. & LaGarry, H. E. in *Depositional environments, lithostratigraphy, and biostratigraphy of the White River and Arikaree groups (late Eocene to early Miocene, North America)* Vol. 325 *Special Paper - Geological Society of America* eds Dennis O. Terry, Hannan E. LaGarry, & Robert M. Hunt, Jr.) 117-141 (Geological Society of America, 1998).

8 Bao, H. M. Purifying synthetic barite for oxygen isotope measurement by dissolution and reprecipitation in a chelating solution. *Analytical Chemistry* 78, 304-309 (2006).

9 Bao, H. M. & Thiemens, M. H. Generation of O_2 from $BaSO_4$ using a CO_2-laser fluorination system for simultaneous analysis of $\delta^{18}O$ and $\delta^{17}O$. *Analytical Chemistry* 72, 4029-4032 (2000).

10 Valley, J. W., Kitchen, N., Kohn, M. J., Niedorf, C. R. & Spicuzza, M. J. UWG-2, a garnet standard for oxygen isotope ratios: strategies for high precision and accuracy with laser heating. *Geochimica et Cosmochimica Acta* 59, 5223-5231 (1995).

11 Edmonds, H. N. & Edmond, J. M. A 3-component mixing model for ridge-creat hydrothermal fluids. *Earth and Planetary Science Letters* 134, 53-67 (1995).

12 Noda, T. & Shimada, K. Water mixing model calculation for evaluation of deep geothermal water. *Geothermics* 22, 165-180 (1993).

13 Tsurumi, M. Self-consistent least-squares method of estimating chemical composition of the sources of chemical contituents in natural waters. *Analytica Chimica Acta* 138, 177-182 (1982).

[14] Van Geen, A. & Boyle, E. Variability of trace-metal fluxes through the Strait of Gibraltar. *Palaeogeography Palaeoclimatology Palaeoecology* 89, 65-79 (1990).

[15] Byun, D. & Schere, K. L. Review of the governing equations, computational algorithms, and other components of the models-3 Community Multiscale Air Quality (CMAQ) modeling system. *Applied Mechanics Reviews* 59, 51-77, doi:10.1115/1.2128636 (2006).

[16] McHenry, J. N. & Dennis, R. L. The relative importance of oxidation pathways and clouds to atmospheric ambient sulfate production as predicted by the regional acid deposition model. *Journal of Applied Meteorology* 33, 890-905 (1994).

[17] Eder, B. & Yu, S. C. A performance evaluation of the 2004 release of Models-3 CMAQ. *Atmospheric Environment* 40, 4811-4824, doi:10.1016/j.atmosenv.2005.08.045 (2006).

[18] Horowitz, L. W. Past, present, and future concentrations of tropospheric ozone and aerosols: Methodology, ozone evaluation, and sensitivity to aerosol wet removal. *Journal of Geophysical Research-Atmospheres* 111, doi:D22211 10.1029/2005jd006937 (2006).

[19] Yarwood, G., Rao, S., Yocke, M. & Whitten, G. Z. Updates to the Carbon Bond chemical mechanism: CB05. *Final Report to the US EPA, RT-0400675 (http://www.camx.com/publ/pdfs/CB05_Final_Report_120805.pdf)* (2005).

[20] Binkowski, F. S. & Roselle, S. J. Models-3 community multiscale air quality (CMAQ) model aerosol component - 1. Model description. *Journal of Geophysical Research-Atmospheres* 108, doi:4183 10.1029/2001jd001409 (2003).

[21] Bhave, P. V. *et al.* in *The 3rd Annual CMAS Models-3 Users' Conference* (Commun. Model. and Anal. Syst.Cent., Chapel Hill, N. C., 18- 20 Oct., 2004).

[22] Yu, S., Bhave, P. V., Dennis, R. L. & Mathur, R. Seasonal and regional variations of primary and secondary organic aerosols over the Continental United States: Semi-empirical estimates and model evaluation. *Environmental Science & Technology* 41, 4690-4697, doi:10.1021/es061535g (2007).

[23] Yu, S. C. *et al.* Evaluation of real-time PM2.5 forecasts and process analysis for PM2.5 formation over the eastern United States using the Eta-CMAQ forecast model during the 2004 ICARTT study. *Journal of Geophysical Research-Atmospheres* 113, doi:D06204 10.1029/2007jd009226 (2008).

[24] Alexander, B., Park, R. J., Jacob, D. J. & Gong, S. L. Transition metal-catalyzed oxidation of atmospheric sulfur: Global implications for the sulfur budget. *Journal of Geophysical Research-Atmospheres* 114, doi:D02309 10.1029/2008jd010486 (2009).

[25] Seinfeld, J. H. & Pandis, S. N. *Atmospheric Chemistry and Physics: From Air Pollution to Climate Change*. (Wiley, 1998).